

NAS-BENCH-301 AND THE CASE FOR SURROGATE BENCHMARKS FOR NEURAL ARCHITECTURE SEARCH

Julien Siems^{1*}, Lucas Zimmer^{1*}, Arber Zela¹, Jovita Lukasik²,

Margret Keuper² & Frank Hutter^{1,3}

¹University of Freiburg, ²University of Mannheim, ³Bosch Center for Artificial Intelligence

{siemsj, zimmerl, zela, fh}@cs.uni-freiburg.de

{jovita, keuper}@uni-mannheim.de

ABSTRACT

Neural Architecture Search (NAS) is a logical next step in the automatic learning of representations, but the development of NAS methods is slowed by high computational demands. As a remedy, several tabular NAS benchmarks were proposed to simulate runs of NAS methods in seconds. However, all existing NAS benchmarks are limited to extremely small architectural spaces since they rely on exhaustive evaluations of the space. This leads to unrealistic results, such as a strong performance of local search and random search, that do not transfer to larger search spaces. To overcome this fundamental limitation, we propose NAS-Bench-301, the first model-based surrogate NAS benchmark, using a search space containing 10^{18} architectures, orders of magnitude larger than any previous NAS benchmark. We first motivate the benefits of using such a surrogate benchmark compared to a tabular one by smoothing out the noise stemming from the stochasticity of single SGD runs in a tabular benchmark. Then, we analyze our new dataset consisting of architecture evaluations and comprehensively evaluate various regression models as surrogates to demonstrate their capability to model the architecture space, also using deep ensembles to model uncertainty. Finally, we benchmark a wide range of NAS algorithms using NAS-Bench-301 allowing us to obtain comparable results to the true benchmark at a fraction of the cost.

1 INTRODUCTION

The successes of deep learning are mainly attributed to its capacity to automatically learn useful feature representations from data, which largely surpassed previous feature engineering approaches. In a similar vein, neural architecture search (NAS) promises to advance the field by removing human bias from architecture design (see, e.g., Elsken et al. (2019b)), achieve new state of the art on many tasks (Real et al., 2019; Chenxi et al., 2019; Saikia et al., 2019) and create resource-aware architectures (Tan et al., 2018; Elsken et al., 2019a; Cai et al., 2020).

At its inception, NAS was shown to be effective in automating the architecture design, but also prohibitively expensive, requiring industry-level compute resources (Zoph & Le, 2017). Since then, research has focused on improving the efficiency of NAS methods. These efforts have introduced the weight-sharing paradigm (Pham et al., 2018) which brought down the cost of NAS to a single GPU day. Many works since then have tried to improve over this paradigm (Liu et al., 2019; Pham et al., 2018; Xu et al., 2020; Dong & Yang, 2019; Zela et al., 2020a; Nayman et al., 2019).

However, empirical evaluations in NAS are still problematic. Different NAS methods often use different training pipelines, perform their search on lower-fidelity proxy models and evaluate the architectures in substantially larger models. In many cases, due to the large computational expense of NAS, the search phase is only run once and the found architecture is evaluated only once. This practice impedes assertions about the statistical significance of the reported results, recently brought into focus by several authors (Yang et al., 2019; Lindauer & Hutter, 2019; Shu et al., 2020; Yu et al., 2020).

*Equal contribution

Recently, several tabular benchmarks (Ying et al., 2019; Zela et al., 2020b; Dong & Yang, 2020; Klyuchnikov et al., 2020) have been proposed to circumvent the aforementioned issues and enable proper scientific evaluations in NAS. However, all of these are severely limited by relying on an exhaustive evaluation of *all* architectures in a search space. This leads to unrealistically small search spaces, so far containing only between 6k and 423k unique architectures, a far shot from standard search spaces used in the NAS literature, which contain more than 10^{18} architectures (Zoph & Le, 2017; Pham et al., 2018; Liu et al., 2019; Cai et al., 2019). Unfortunately, this discrepancy in search spaces leads to very different characteristics of existing NAS benchmarks and realistic NAS search spaces that limit the conclusions that can be drawn from existing NAS benchmarks: for example, local search yields the best available results in existing NAS benchmarks but performs poorly in realistic search spaces (White et al., 2020b), such as the one used by DARTS (Liu et al., 2019).

To address these problems, we make the following contributions:

1. We present *NAS-Bench-301*, a surrogate NAS benchmark that is first to cover a realistically-sized search space (namely the cell-based search space of DARTS (Liu et al., 2019)), containing more than 10^{18} possible architectures. As a surrogate benchmark, rather than having to exhaustively evaluate every architecture, NAS-Bench-301 deploys a surrogate model trained on function evaluations to cover this large search space.
2. Using *NAS-Bench-101* (Ying et al., 2019), we show that a surrogate benchmark fitted on a subset of the architectures in the search space can in fact model the true performance of architectures *better* than a tabular NAS benchmark.
3. We analyze and release NAS-Bench-301 as a dataset consisting of $\sim 50k$ architecture evaluations that will also be publicly available in the Open Graph Benchmark (OGB) (Hu et al., 2020) for evaluating other NAS performance predictors. We evaluate a variety of regression models fitted on said dataset as surrogate candidates and show that it is possible to accurately predict the performance of architectures sampled from previously-unseen and extreme regions of the architecture space.
4. We utilize NAS-Bench-301 as a benchmark for running black-box (discrete) optimizers resulting in a large speedup over the true benchmark since each architecture evaluation takes less than a second to query from the surrogate, compared to 1-2 hours for training an architecture. We show that the resulting search trajectories on the surrogate benchmark closely resemble groundtruth trajectories. In contrast to the much smaller existing NAS-Benchmarks, we can demonstrate that random search is not a competitive baseline on our realistic search space.

We hope that NAS-Bench-301 will facilitate statistically sound yet realistic benchmarking of NAS methods. In order to foster reproducibility, we open-source all the code and data in the following repository: <https://github.com/automl/nasbench301>.

2 MOTIVATION – CAN WE DO BETTER THAN A TABULAR BENCHMARK?

In this section, we expose an issue of tabular benchmarks that has largely gone unnoticed and go on to show that surrogate benchmarks can provide *better* performance estimates than tabular benchmarks based on *less* data.

Tabular NAS benchmarks are built around a costly, exhaustive evaluation of *all* possible architectures in a search space, and when a particular architecture’s performance is queried, the tabular benchmark simply returns the respective table entry. The issue with this process is that, due to the stochasticity of SGD training, the result of evaluating the error of architecture i is a random variable X_i , and in the table we only save the result of a single draw $x_i \sim X_i$ (or a very small number of draws we can afford to run for each architecture; existing NAS benchmarks have up to 3 runs per architecture).

Given that there is noise in the evaluations, if we have one or more evaluations available for each of the architectures in a search space, from a statistical perspective, one may then view a tabular NAS benchmark as a simple estimator that assumes the performance of all architectures to be entirely *independent* of each other, and thus estimates the error of an architecture based only on previous evaluations of this exact architecture. However, from a machine learning perspective, knowing that similar architectures tend to yield similar performance, and knowing that the variance of individual evaluations can be high (both described, e.g., in NAS-Bench-101 (Ying et al., 2019)), one may

wonder whether one can construct better estimators. Indeed, this is precisely the supervised learning problem of performance prediction in the space of neural architectures (see Section 7.2 for related work on this problem), and, so, under this view it should not come as a surprise that a learned regression model can show lower estimation error than tabular benchmarks. In the remainder of this section, we show a concrete example where this is the case.

Setup for Proof of Concept Experiment. We chose NAS-Bench-101 (Ying et al., 2019) for our analysis, because it contains 3 evaluations per architecture (on the full 108 epoch budget). Given the validation accuracies y_1, y_2, y_3 of the three evaluations for each architecture, we trained a surrogate model on a single seed of each architecture in NAS-Bench-101, e.g. $y_{\text{train}} = y_1$. If the surrogate model learns to smooth out the noise, then the Mean Absolute Error (MAE) between the predicted validation accuracy y_{pred} to the average validation accuracy of the two remaining seeds, in this case $y_{\text{test}} = \bar{y}_{23}$, should be smaller than the MAE of the validation accuracy of y_1 to \bar{y}_{23} .

We emphasize that training a surrogate to model a search space differs from a typical regression task in that it represents a transductive inference task. By definition of the search space, the set of possible architectures is known ahead of time (although it may be very large), hence a surrogate model does not have to generalize to out-of-distribution data if the training data covers the space well.

Many possible models can be used as surrogates (see the related work in Section 7.2); here, we chose a graph convolutional network (GCN), specifically, a GIN model (Xu et al., 2019a) (as implemented by Errica et al. (2020)). We successively increase the amount of training data up to the full data for one seed of NAS-Bench-101 ($\sim 400\text{k}$ unique architectures). Following Wen et al. (2019); Friede et al. (2019), we excluded the diverged models contained in NAS-Bench-101 by removing models which obtained less than 50% validation accuracy on any of the three evaluations. Finally, we evaluated the GIN and the tabular benchmark (both based on one seed) on the remaining two seeds (y_{test}). For training details we refer to Appendix A.1.1.

Results of Proof of Concept Experiment. Table 1 compares the error between the surrogate model when trained on one seed of all architectures and the tabular benchmark. For all possible choices of training seeds, the surrogate model yields a lower MAE than the tabular benchmark.¹

Figure 1 depicts how the GIN scales with different percentages of training data. Only when the ratio of training data for the GIN surrogate model decreases below 5% of all data in NAS-Bench-101 (i.e. $\sim 21,500$ architectures), does the surrogate model perform worse than the tabular benchmark. We note that this analysis is done with the same hyperparameter setting for all ratios of training data. Hence, the surrogates could require even less training data to reach similar performance to the tabular benchmark if the hyperparameters were tuned on every level.

From this proof of concept, we conclude that a surrogate model *can* yield strong performance when only a subset of the search space is available as training data (and can in the extreme even outperform a tabular benchmark by smoothing out the noise in the architecture evaluation). This opens up a garden of delights, as it allows us to create NAS benchmarks for arbitrary NAS spaces, in particular much larger, realistic ones, for which it is completely infeasible to create an exhaustive tabular benchmark. In the remainder of the paper, we will focus on creating such a surrogate benchmark,

Model Type	Mean Absolute Error (MAE)		
	2, [0, 1]	1, [0, 2]	0, [1, 2]
Tabular	4.539e-3	4.546e-3	4.534e-3
Surrogate	3.441e-3	3.455e-3	3.446e-3

Table 1: Mean absolute error between the predicted validation accuracy for two of the three evaluations per configuration and the remaining configuration’s validation accuracy. Test seeds are denoted in brackets.

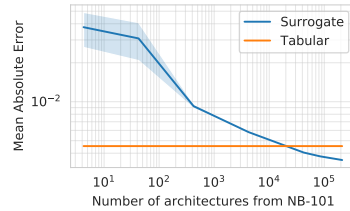


Figure 1: Number of architectures used for training the GIN surrogate model vs MAE on the NAS-Bench-101 dataset.

¹We do note that the average estimation error of tabular benchmarks could be reduced by a factor of \sqrt{k} by performing k runs for each architecture. The error of a surrogate model would also shrink when the model is based on more data, but as k grows large the independence assumption of tabular benchmarks would become competitive with surrogate models.

Optimizer		# Evaluations
Discrete	RS	24047
	Evolution	DE 7275
		RE 4639
	BO	TPE 6741
		BANANAS 2243
One-Shot	COMBO	745
	DARTS	2053
	GDAS	234
	RANDOM-WS	198
	PC-DARTS	149

Table 2: Overview of the optimizers used to cover the search space.

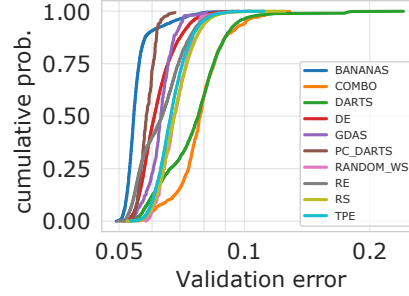


Figure 2: Empirical Cumulative Density Function (ECDF) plot comparing all optimizers in the dataset. Optimizers which cover good regions of the search space will have higher cumulative prob in the low validation error region.

NAS-Bench-301, for the most frequently used NAS search space: the one used by DARTS (Liu et al., 2019).

3 THE NAS-BENCH-301 DATASET

In this section, we describe the *NAS-Bench-301* dataset of over 50k architectures and their performances. Next to its use in order to create the *NAS-Bench-301* surrogate NAS benchmark later on in this paper, this dataset allows us to gain various insights (e.g., which types of architectures are being explored by different NAS methods, and what are the characteristics of architectures that work well) and it is also relevant to the Graph Learning community, since it offers a challenging graph space with noisy evaluations per graph as they may be encountered in practice. To encourage transparency and reproducibility, we are collaborating with the Open Graph Benchmark (OGB) (Hu et al., 2020) to offer a public leaderboard.

3.1 SEARCH SPACE

We use the same architecture search space as in DARTS (Liu et al., 2019). Specifically, the normal and reduction cell each consist of a DAG with 2 input nodes (receiving the output feature maps from the previous and previous-previous cell), 4 intermediate nodes (each adding element-wise feature maps from two previous nodes in the cell) and 1 output node (concatenating the outputs of all intermediate nodes). Input and intermediate nodes are connected by directed edges representing one of the following operations: {Sep. conv 3×3 , Sep. conv 5×5 , Dil. conv 3×3 , Dil. conv 5×5 , Max pooling 3×3 , Avg. pooling 3×3 , Skip connection}.

3.2 DATA COLLECTION

Since the DARTS search space we consider is too large to exhaustively evaluate, a central question in our design was how to decide which architectures to include to achieve a good coverage of the overall architecture space while also providing a special focus on well-performing regions that optimizers tend to explore more. Our principal methodology is inspired by Eggenberger et al. (2015), who balanced unbiased collection by uniform random sampling for good overall coverage with biased and dense data collection in high-performance regions by running hyperparameter optimizers. This is desirable for a surrogate benchmark since we are interested in well-performing optimizers that explore well-performing regions.

Following this approach, we evaluated over 25k randomly sampled architectures and added architectures found by the following nine optimizers. We used Tree-of-Parzen-Estimators (TPE) (Bergstra et al., 2011) as implemented by Falkner et al. (2018) as a baseline BO method. Since several recent works have proposed to apply BO over combinatorial spaces (Oh et al., 2019; Baptista & Poloczek, 2018) we also used COMBO (Oh et al., 2019). We included BANANAS (White et al., 2019) as our third BO method, which uses a neural network with a path-based encoding as a surrogate model

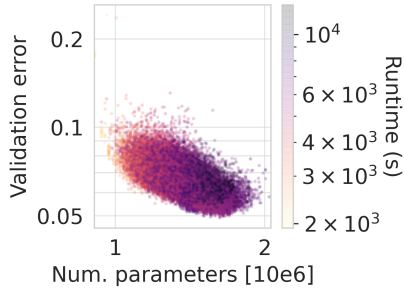


Figure 3: Number of parameters against validation error with model training time as colorbar.

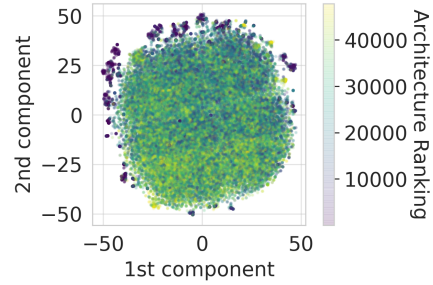


Figure 4: t-SNE visualization of the sampled architectures colored as ranked w.r.t their validation accuracy.

and hence scales better with the number of function evaluations. As two representatives of evolutionary approaches to NAS we chose Regularized Evolution (RE) (Real et al., 2019) as it is still one of the state-of-the-art methods in discrete NAS and Differential Evolution (Price et al., 2006) as implemented by Awad et al. (2020). Accounting for the surge in interest in One-Shot NAS, our data collection also entails evaluation of architectures from the search trajectory of DARTS (Liu et al., 2019), GDAS (Dong & Yang, 2019), RANDOM-WS (Li & Talwalkar, 2019) and PC-DARTS (Xu et al., 2020). For details on the setup of each NAS optimizer and the architecture training details we refer to Appendices A.3 and A.4, respectively.

In total, our dataset \mathcal{D} consists of around 50,000 data points, broken down into the optimizers they originate from in Table 2. For each architecture $\lambda \in \Lambda$, the dataset contains the following metrics: train/validation/test accuracy, training time and number of model parameters.

3.3 ARCHITECTURE SPACE COVERAGE

We now perform an in-depth exploration of how the different NAS optimizers cover the search space. The trajectories from the different NAS optimizers yield quite different performance distributions. This can be seen in Figure 2 which shows the ECDF of the validation errors of the architectures evaluated by each optimizer. As the computational budgets allocated to each optimizer vary widely, this data does not allow for a fair comparison between the optimizers. However, it is worth mentioning that the evaluations of BANANAS were focused on the best architectures, followed by PC-DARTS, DE, GDAS, and RE. TPE only evaluated marginally better architectures than RS, while COMBO and DARTS evaluated the worst architectures.

To visualize the coverage of the search space further, we performed a t-distributed Stochastic Neighbor Embedding (t-SNE) (Maaten & Hinton, 2008) on the categorical architecture space, see Figure 4. Besides showing a good overall coverage, some well-performing architectures in the search space form distinct groups which are mostly located outside the main cloud of points. Similarly, we performed a t-SNE visualization for each optimizer in a common t-SNE projection, demonstrating that the different optimizers evaluate very different types of architectures (see Figure 12 in the appendix).

3.4 PERFORMANCE STATISTICS

Figure 3 studies the interplay between validation errors, model parameters, and runtime. Generally, as expected, models with more parameters are more costly to train but achieve lower validation error.

Training and test errors are highly correlated with a Kendall tau rank correlation of $\tau = 0.845$ (Spearman rank corr. 0.966), minimizing the risk of overfitting on the validation error.

NAS-Bench-301 also avoids some shortcomings of NAS-Bench-101 and NAS-Bench-201 w.r.t. to the training pipelines. In both NAS-Bench-101 and NAS-Bench-201 the training accuracy of many of the evaluated architectures reaches 100% which is unrealistic in most practical settings, because it is avoided by data augmentation techniques which are commonplace as data is usually scarce. In NAS-Bench-201 the test error appears shifted higher compared to the validation error, pointing to other shortcomings in their training pipeline. Our training pipeline described in detail section A.4,

avoids these failures by utilizing many modern data augmentation techniques, leading to a more realistic assessment of the architectures.

3.5 CELL TOPOLOGY AND OPERATIONS

We now analyze the collected dataset for NAS-Bench-301 to gain some understanding of the influence of the cell topology and the operations on the performance of the architectures in the DARTS search space in our setting. The discovered properties of the search space then inform our choice of metrics for the evaluation of different surrogate models.

We now study how validation error depends on the depth of architectures. Figure 5 visualizes the performance distribution for the normal and reduction cell depth² via violin plots which approximate empirical distributions with a kernel density estimation (Hwang et al., 1994). From the plot we can infer that the performance distributions for the normal and reduction cell are similar for the same cell depth. Although cells of all depths can reach high performances, shallower cells seem slightly favored. Note that these observations are subject to changes in the hyperparameter setting, e.g. training for more epochs may render deeper cells more competitive. The best found architecture has a normal and reduction cell of depth 4. We also show the distribution of normal and reduction cell depths evaluated by each optimizer in Figure 14 in the appendix.

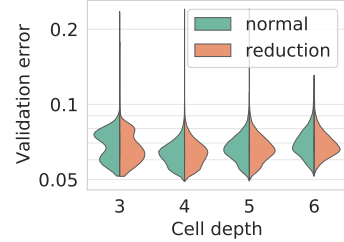


Figure 5: Distribution of the validation error for different cell depth.

The DARTS search space contains operation choices without parameters such as Skip-Connection, Max Pooling 3×3 and Avg Pooling 3×3 . We visualize the influence of these parameter-free operations on the validation error in the normal cell in Figure 7a. For the reduction cell we refer to Figure 15 in the appendix. While pooling operations in the normal cell seem to have a negative impact on performance, a small number of skip connections improves overall performance. This is somewhat expected, since the normal cell is dimension preserving and skip connections help training by improving gradient flow like in ResNets (He et al., 2016). For both cells, having many parameter-free operations significantly deteriorate performance. We therefore would expect that a good surrogate also models this case as a poorly performing region.

3.6 NOISE IN ARCHITECTURE EVALUATIONS

As discussed in Section 2, the noise in architecture evaluations can be large enough for surrogate models to yield more realistic estimates of architecture performance than tabular benchmark based on a single evaluation per architecture. To study the magnitude of this noise for NAS-Bench-301, we evaluated 500 architectures randomly sampled from our DE run with 5 different seeds.³ We also include other architectures that were evaluated at least 5 times during the optimizer runs.

We find a mean standard deviation of $1.7e - 3$ for the final validation accuracy which is slightly less than the noise observed in NAS-Bench-101 (Ying et al., 2019). Figure 6 shows that, while the noise tends to be lower for the best architectures, a correct ranking would still be hard based on a single evaluation. Finally, we compare the MAE when estimating architecture performance from only one sample to the results from Table 1. On the larger search space and with more evaluations we find an MAE of $1.2e - 3$ which is also slightly lower than found in NAS-Bench-101, one reason possibly being a more robust training pipeline.

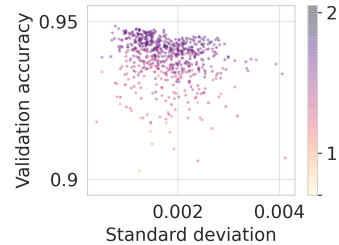


Figure 6: Standard deviation of the validation accuracy for multiple architecture evaluations.

²We follow the definition of cell depth used by Shu et al. (2020), i.e. the length of the longest simple path through the cell.

³We chose DE because it exhibits good exploration while achieving good performance, see Figure 12 in the appendix.

4 FITTING SURROGATE MODELS ON THE NAS-BENCH-301 DATASET

In this section, we fit and evaluate a wide range of surrogate models to the NAS-Bench-301 dataset. The predictions of any such regression model give rise to a surrogate NAS benchmark, but models that fit the true performance better can of course be expected to give rise to surrogate NAS benchmarks whose characteristics are more similar to the ones of the original (non-surrogate) NAS benchmark. Therefore, naturally, we strive for the best-fitting model. We emphasize that we do not attempt to introduce a new regression model but rather build on the shoulders of the architecture performance prediction community. As the state-of-the-art in this field improves, our surrogate NAS benchmarks will only get *better*, and in order to facilitate progress along these lines, we are collaborating with the Open Graph Benchmark (OGB) (Hu et al., 2020) to offer a public leaderboard.

The metrics we chose to evaluate different surrogate models take into account our goal of creating surrogate NAS benchmarks whose characteristics resemble the original (non-surrogate) NAS benchmark they are based on. They include simple correlation statistics between predicted and true performance of architectures, correlation statistics when evaluating on architectures sampled by a new NAS optimizer not used for data collection, as well as qualitative evaluations of the model’s behaviour when changing the cell topology and number of parameters. We also ensemble regressors to obtain a predictive distribution and compare to the noise observed on groundtruth data. Finally, in the next section, we will also study the actual resemblance of NAS optimizers’ trajectories on the surrogate and original NAS benchmarks.

4.1 SURROGATE MODEL CANDIDATES

Deep Graph Convolutional Neural Networks are frequently used as NAS predictors (Friede et al., 2019; Wen et al., 2019; Ning et al., 2020; Dwivedi et al., 2020). In particular, we choose the GIN since several works have found that it performs well on many benchmark datasets (Errica et al., 2020; Hu et al., 2020). We use the publicly available implementation from the Open Graph Benchmark (Hu et al., 2020). This implementation uses virtual nodes (additional nodes which are connected to all nodes in the graph) to boost performance as well as generalization and consistently achieves good performance on their public leaderboards. Other GNNs from Errica et al. (2020), such as DGCNN and DiffPool, performed worse in our initial experiments and are therefore not considered.

Following recent work in Predictor-based NAS (Ning et al., 2020; Xu et al., 2019b), we use a per batch ranking loss, because the ranking of an architecture is equally important to an accurate prediction of the validation accuracy in a NAS setting. We use the ranking loss formulation by GATES (Ning et al., 2020) which is a hinge pair-wise ranking loss with margin $m=0.1$.

We compare the GIN to a large variety of regression models commonly used in Machine Learning. We evaluate Random Forests (RF) and Support Vector Regression (SVR) using implementations from Pedregosa et al. (2011). In addition, we compare with the tree-based gradient boosting methods XGBoost (Chen & Guestrin, 2016) and LGBBoost (Ke et al., 2017), which have recently been used for predictor-based NAS (Luo et al., 2020).

4.2 EVALUATING THE DATA FIT

Similarly to Wen et al. (2019); Baker et al. (2017) we assess the quality of the data fit via the coefficient of determination (R^2) and the Kendall rank correlation coefficient (τ). However, Kendall τ is sensitive to noisy evaluations that change the rank of an architecture. Therefore, we follow the recent work by Yu et al. (2020) and use a sparse Kendall Tau (sKT), which ignores rank changes at 0.1% accuracy precision, by rounding the predicted validation accuracy prior to computing the Kendall Tau.

All hyperparameters of the models were tuned using BOHB (Falkner et al., 2018) as a black-box optimizer. Details on the hyperparameter search spaces for the respective surrogate models are given in Table 6 in the ap-

Model	Validation		Test	
	R^2	sKT	R^2	sKT
GIN	0.809	0.787	0.804	0.782
BANANAS	0.697	0.699	0.703	0.691
XGBoost	0.890	0.821	0.886	0.820
LGBBoost	0.893	0.824	0.894	0.814
NGBoost	0.793	0.753	0.797	0.751
RF	0.609	0.676	0.651	0.666
ϵ -SVR	0.687	0.678	0.676	0.665
μ -SVR	0.685	0.665	0.675	0.662

Table 3: Coefficient of determination R^2 and sparse Kendall- τ rank correlation coefficient for different regression models used as surrogates.

	Model	No RE	No DE	No COMBO	No TPE	No BANANAS	No DARTS	No PC-DARTS	No GDAS	No RANDOM-WS
R^2	GIN	0.311	0.822	0.789	0.778	0.780	0.157	0.468	0.328	0.729
	LGB	0.928	0.884	0.921	0.854	0.862	-0.027	0.390	0.487	0.903
	XGB	0.919	0.884	0.881	0.838	0.893	-0.104	0.430	0.682	0.949
sKT	GIN	0.806	0.756	0.752	0.716	0.542	0.713	0.467	0.575	0.771
	LGB	0.828	0.781	0.838	0.769	0.539	0.774	0.484	0.591	0.844
	XGB	0.826	0.776	0.823	0.759	0.546	0.780	0.468	0.653	0.917

Table 4: Leave One-Optimizer-Out analysis results for a selection of the analyzed surrogate models.

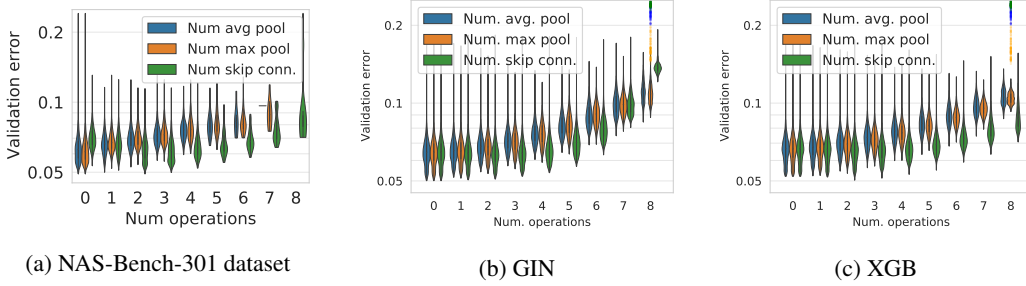


Figure 7: (Left) Distribution of validation error in dependence of the number of parameter-free operations in the normal cell on the NAS-Bench-301 dataset. (Middle and Right) Predictions of each surrogate model for the increase in no-parameter operations. The collected groundtruth data is shown as scatter plot. Violin plots are cut off at the respective observed minimum and maximum value.

pendix. We train using train/val/test splits (0.8/0.1/0.1) stratified on the optimizers used for the data collection. We provide additional details on the preprocessing of the architectures for the surrogate models in Appendix A.2. As Table 3 shows, the three best performing models were LGB, XGB and GIN; we therefore focus our analysis on these in the following.

4.3 LEAVE ONE-OPTIMIZER-OUT ANALYSIS

Since the aim of NAS-Bench-301 is to allow efficient benchmarking of novel NAS algorithms, it is necessary to ensure that the surrogate model can deliver accurate performances on trajectories by unseen optimizers. Similarly to Eggenberger et al. (2015), we therefore perform a form of cross-validation on the optimizers we used for data collection. For this analysis we train the surrogate model on the data from all but one optimizer (using a stratified 0.9/0.1 train/val split over the optimizers). Then we predict the unseen results from the left-out optimizer to evaluate how well the models extrapolate to the region covered by the 'unseen' optimizer. We refer to this as the leave-one-optimizer-out (LOOO) setting.

Results Table 2 shows the results for GIN, LGB and XGB. Overall, the rank correlation between the predicted and observed validation accuracy remains high even when a well-performing optimizer such as RE is left out. Leaving out BANANAS decreases the rank correlation, however the high R^2 measure shows that the fit is good and the decrease in rank correlation can be explained by the optimization of the acquisition function (which is based on mutating already found architectures).

The One-Shot optimizers PC-DARTS and GDAS appear the most challenging to predict in our setting, however these are also the optimizers for which we have collected the fewest amount of data (Table 2) and we are planning to include more architectures found by these optimizers in the near future.

4.4 PARAMETER-FREE OPERATIONS

Several works have found that methods based on DARTS (Liu et al., 2019) are prone to finding sub-optimal architectures that contain many, or even only, parameter-free operations (max. pooling, avg. pooling or skip connections) and perform poorly (Zela et al., 2020a; Xu et al., 2020; Dong &

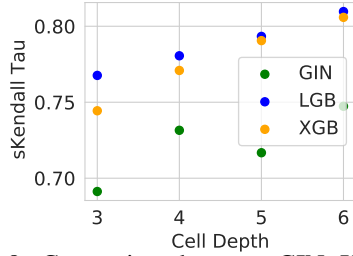


Figure 8: Comparison between GIN, XGB and LGB on the cell topology analysis.

Model Type	MAE 1, [2, 3, 4, 5]	Mean σ	KL divergence
Tabular	$1.66e-3$	$1.7e-3$	undefined
GIN	$1.64e-3$	$1.2e-3$	3.2
LGB	$1.44e-3$	$0.3e-3$	63.1
XGB	$1.46e-3$	$0.3e-3$	113.9

Table 5: Metrics for the selected surrogate models on 500 architectures from our DE run that were evaluated 5 times.

Yang, 2020). The surrogate models are evaluated by replacing a random selection of operations in a cell with one type of parameter-free operations to match a certain ratio of parameter-free operations in a cell. This analysis is carried out over the test set of the surrogate models and hence contains architectures collected by all optimizers. For a more robust analysis, for each ratio of operations to replace, we repeated this experiment 4 times.

Results Figure 7 shows that both the GIN and the XGB model correctly predict that accuracy drops with too many parameter-free operations, especially for skip connections. The groundtruth of architectures with only parameter-free operations is displayed as scatter plot. Out of the two models, XGB better captures the slight performance improvement of using a few skip connections. LGB failed to capture this trend but performed very similarly to XGB for the high number of parameter-free operations.

4.5 CELL TOPOLOGY ANALYSIS

We now analyze how well changes in the cell topology (rather than in the operations) are modeled by the surrogates. We collected groundtruth data by evaluating all $\prod_{k=1}^4 \frac{(k+1)k}{2} = 180$ different cell topologies (not accounting for isomorphisms) with fixed sets of operations. We assigned the same architecture to the normal and reduction cell, to focus on the effect of the cell topology. We sampled 10 operation sets uniformly at random, leading to 1800 architectures as groundtruth for this analysis.

We evaluate all architectures and group the results based on the cell depth. For each of cell depths we then compute the sparse Kendall τ rank correlation between the predicted and true validation accuracy.

Results Results of the cell topology analysis are shown in Figure 8. We observe that LGB slightly outperforms XGB, both of which perform better on deeper cells. The GIN performs worst, but manages to capture the trend towards better performance for deeper cells.

4.6 NOISE MODELLING

Ensemble methods are commonly used to improve predictive performance (Dietterich, 2000). Moreover, ensembles of deep neural networks, so-called deep ensembles, have been proposed as a simple way to additionally obtain predictive uncertainty (Lakshminarayanan et al., 2017). We therefore create an ensemble of 10 base learners for each of our three best performing models (GIN, XGB, LGB) using a 10-fold cross-validation for our train and validation split and different initializations.

We use the architectures with multiple evaluations (see Section 3.6) to perform a similar study as in Section 2. We train an ensemble of surrogate models, using only one evaluation per architecture (i.e., seed 1) and take the mean accuracy of the remaining ones as groundtruth (i.e., seeds 2-5). We compare against a tabular model with just one evaluation (seed 1). Table 5 shows that the surrogate models yield estimates closer to groundtruth than the table lookup based on one evaluation. This confirms our main finding from Section 2, but this time on a much larger search space.

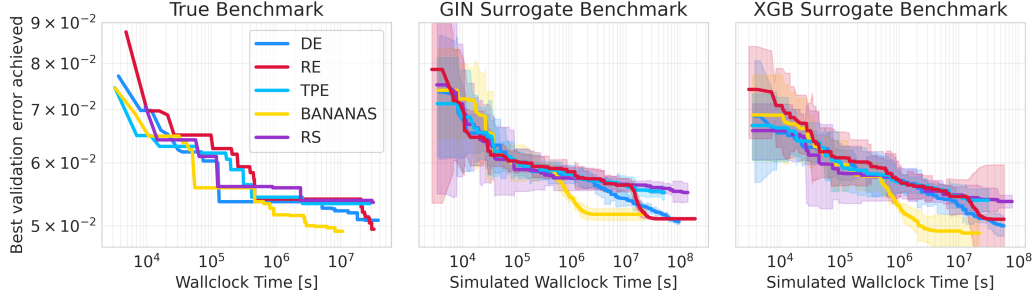


Figure 9: Anytime performance of different optimizers on the real benchmark (left) and the surrogate benchmark (GIN (middle) and XGB (right)) when training ensembles on data from collected from all optimizers. Trajectories on the surrogate benchmark are averaged over 5 runs.

We also compare the predictive distribution of our ensembles to the groundtruth. To that end, we assume normally distributed data and compute the KullbackLeibler divergence (KL divergence) between the groundtruth accuracy distribution and predicted distribution. We report the results in Table 5. The GIN ensemble provides the closest estimate to the real distribution with a KL divergence of 3.2 and a mean standard deviation of 1.2×10^{-3} which is closer to the groundtruth than LGB and XGB.

5 ANALYZING NAS-BENCH-301 AS A NAS BENCHMARK

Having assessed the quality of the surrogate models on modeling the search space, we now use NAS-Bench-301 to benchmark various NAS algorithms.

In addition to predicting the validation accuracy, it is necessary to predict the runtime of an architecture evaluation. This is achieved by training an LGB model with the runtime as targets. We performed a separate HPO to obtain our runtime model (for details, see Appendix A.6.1).

5.1 USING ALL DATA

We first compare the trajectories on the true benchmark and on the surrogate benchmark when training the surrogate on all data. For the true benchmark, we show the trajectories contained in our dataset (based on a single run, since we could not afford repetitions due to the extreme compute requirements of $> 10^7$ seconds, i.e., 115 days, of GPU time for a single run). For the evaluations on the surrogate, in contrast, we can trivially afford to perform multiple runs and provide error bars. For the surrogate trajectories, we use an identical initialization for the optimizers (e.g. initial population for RE) but evaluations of the surrogate benchmark are done by sampling from the surrogate model’s predictive distribution for the architecture at hand, leading to different trajectories.

Results As Figure 9 shows, both the XGB and the GIN surrogate capture behaviors present on the true benchmark. For instance, the strong improvements of BANANAS and RE are also present on the surrogate benchmark at the correct time. In general, the ranking of the optimizers towards convergence is accurately reflected on the surrogate benchmark. Also the initial random exploration of algorithms like TPE, RE and DE is captured as the large initial variation in performance indicates. Notably, the XGB surrogate exhibits a high variation in well-performing regions as well and seems to slightly underestimate the error of the best architectures. The GIN surrogate, on the other hand, shows less variance in these regions but slightly overpredicts for the best architectures.

An important feature of both the true and surrogate benchmark is the bad performance of random search. Due to the size of the search space, random search is clearly outmatched by other algorithms even after many evaluations, with BANANAS finding the best architectures orders of magnitude faster. This stands in contrast to previous NAS benchmarks. For instance, NAS-Bench-201 (Dong & Yang, 2020) only contains 6466 architectures in total, causing the median of random search runs to find the best architecture after only 3233 evaluations.

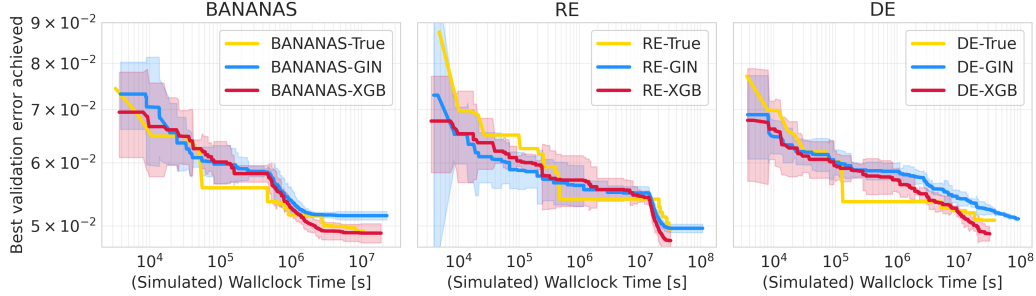


Figure 10: Anytime performance of different optimizers on the real benchmark and the surrogate benchmark when using ensemble surrogate models without data from trajectories of the optimizer under consideration.

5.2 LEAVE ONE-OPTIMIZER-OUT

To simulate benchmarking of novel algorithms, we expand on the leave one optimizer out analysis from Section 4.3 by benchmarking optimizers with surrogate models that have not seen data from their trajectories. We again compare the trajectories obtained from 5 runs on the surrogate benchmark to the groundtruth.

Results Figure 10 shows the trajectories in the leave-one-optimizer-out setting. The XGB and GIN surrogates again capture the general behavior of different optimizers well, illustrating that characteristics of new optimization algorithms can be captured with the surrogate benchmark.

6 GUIDELINES FOR USING NAS-BENCH-301 AND SURROGATE BENCHMARKS

To ensure realistic and fair benchmarking of NAS algorithms, we recommend certain best practices. This is particularly important for a surrogate benchmark, since abusing knowledge about the surrogate model can lead to the design of algorithms that overfit to the surrogate benchmark. The following provides a checklist, for clean benchmarking on NAS-Bench-301:

- The surrogate model should be treated as a black-box function and hence only be used for querying. We strongly discourage approaches which e.g. use gradients with respect to the input graphs to search directly within the embedding space created by our surrogates models as this would likely lead to overfitting to our benchmark.
- We only recommend using surrogate models whose characteristics match those of the true benchmark as closely as possible. So far, we make available three surrogate NAS benchmarks, using our LGB, XGB, and GIN models.
- We will collect more training data, which will further improve the model fits. Because of this, to preserve comparability of results in different published papers, we believe version numbers are crucial. So far, we release NB301-LGB-v0.9, NB301-XGB-v0.9, and NB301-GIN-v0.9.

We encourage the community to propose a wide range of additional surrogate NAS benchmarks, using different search spaces, datasets, and problem domains. We encourage the creators of such NAS benchmarks to follow the same principles we followed to gather data from random configurations and a broad range of state-of-the-art architectures, and to check their predictions both qualitatively and quantitatively.

7 RELATED WORK

7.1 EXISTING NAS BENCHMARKS

Benchmarks for NAS were introduced only recently with NAS-Bench-101 (Ying et al., 2019) as the first among them. NAS-Bench-101 is a tabular benchmark consisting of $\sim 423k$ unique architectures

in a cell structured search space evaluated on CIFAR-10 (Krizhevsky, 2009). To restrict the number of architectures in the search space, the number of nodes and edges was restricted and only three operations are considered. One result of this limitation is that One-Shot NAS methods can only be applied to subspaces of NAS-Bench-101, given in NAS-Bench-1Shot1 (Zela et al., 2020b).

NAS-Bench-201 (Dong & Yang, 2020), in contrast, uses a search space with a fixed number of nodes and edges, hence allowing for a straight-forward application of one-shot NAS methods. However, its search space only has 4 intermediate nodes, limiting the total number of unique architectures to as few as 6466. NAS-Bench-201 includes evaluations of all these architectures on three different datasets, namely CIFAR-10, CIFAR-100 (Krizhevsky, 2009) and Downsampled Imagenet 16×16 (Chrabaszcz et al., 2017), therefore allowing for transfer learning experiments.

NAS-Bench-NLP (Klyuchnikov et al., 2020) was recently proposed as a tabular benchmark for NAS in the Natural Language Processing domain. The search space closely resembles NAS-Bench-101 by limiting the number of edges and nodes to constrain the search space size resulting in over 14k evaluated architectures.

Recent works have shown that search spaces offered by current NAS benchmarks and search spaces typically used to perform NAS for deployment exhibit significantly different characteristics. For instance, local search achieves state-of-the-art results on current benchmarks but performs poorly on the search space used by DARTS (White et al., 2020b). Our proposed NAS-Bench-301 differs from previous NAS benchmarks in that it covers a significantly larger search space. We overcome this limitation by proposing the first surrogate benchmark for NAS that allows coverage of the full DARTS search space.

7.2 NEURAL NETWORK PERFORMANCE PREDICTION

There exist several works on predicting NN performance based on their neural architecture, training hyperparameters, and initial performance. Domhan et al. (2015) used MCMC to extrapolate performance only from the initial learning curve, while Klein et al. (2017) constructed a Bayesian NN for learning curve prediction that also includes architectural features and hyperparameters; Baker et al. (2017) used traditional regression models to predict final performance based on an initial learning curve and architectural features.

A more recent line of work in performance prediction focuses more on the featurized representation of neural architectures. Peephole (Deng et al., 2017) considers only forward architectures and aggregate the information about the operations in each layer using an LSTM. Similarly, TAPAS (Isstrate et al., 2019) uses an encoding like Peephole but extends the framework to deal with multiple datasets following the life-long learning setting. An interesting alternative route to represent neural architectures was taken by BANANAS (White et al., 2019) which introduced a path-based encoding of cells that automatically resolves the computational equivalence of two architectures and used it to train a performance predictor to guide Bayesian optimization.

Graph Neural Networks (GNNs) (Gori et al., 2005; Kipf & Welling, 2017; Zhou et al., 2018; Wu et al., 2019) with their capability of learning representations of graph-structured data appear to be a natural choice to learning embeddings of NN architectures. Shi et al. (2019) and Wen et al. (2019) trained a Graph Convolutional Network (GCN) on a subset of NAS-Bench-101 (Ying et al., 2019) showing its effectiveness in predicting the performance of unseen architectures. Moreover, Friede et al. (2019) propose a new variational-sequential graph autoencoder (VS-GAE) which utilizes a GNN encoder-decoder model in the space of architectures and generates valid graphs in the learned latent space.

Several recent works further adapt the GNN message passing to embed architecture bias via extra weights to simulate the operations such as in GATES (Ning et al., 2020) or integrate additional information on the operations (e.g. flop count) (Xu et al., 2019b).

An interesting alternative route was taken by Tang et al. (2020) who operate GNNs on relation graph based on architecture embeddings in a metric learning setting allowing them to pose NAS performance prediction in a semi-supervised setting.

We use methods from NN performance prediction to create our surrogate model. By making our NAS-Bench-301 training dataset publicly available, we hope to foster benchmarking of performance

prediction methods via the Open Graph Benchmark (OGB) (Hu et al., 2020) interface. Since our surrogate NAS benchmark is not committed to a certain performance prediction method, future advances in this field can also yield improvements of our surrogate benchmark.

8 CONCLUSION & FUTURE WORKS

We proposed NAS-Bench-301, the first surrogate benchmark for Neural Architecture Search and first to cover the full, popular DARTS search space with 10^{18} architectures which is orders of magnitude larger than all previous NAS benchmarks. Our new benchmark addresses the challenge of benchmarking NAS methods on realistic search spaces, caused by the computational burden of fully training an architecture, by replacing the evaluation of an architecture with querying a surrogate model. We collected data on the DARTS search space by running multiple optimizers on it, including random search, and explored the resulting dataset. We used this dataset to train and compare different regressor models to serve as surrogate model. Finally, we have demonstrated our surrogate benchmark to accurately and cheaply recover characteristics of different state-of-the-art NAS optimizers found on the true DARTS search space at a fraction of the cost. We hope that NAS-Bench-301 can provide a cheap, yet realistic benchmark to compare new NAS optimizers and allow for fast prototyping. We expect more surrogate benchmarks to be introduced in the future which we expressly welcome.

REFERENCES

- Proceedings of the International Conference on Learning Representations (ICLR'17)*, 2017. Published online: iclr.cc.
- Noor Awad, Neeratyoy Mallik, and Frank Hutter. Differential evolution for neural architecture search (dehb). In *International Conference on Machine Learning (ICLR) Neural Architecture Search (NAS) Workshop*, 2020.
- Bowen Baker, Otakrist Gupta, Ramesh Raskar, and Nikhil Naik. Accelerating Neural Architecture Search using Performance Prediction. In *NIPS Workshop on Meta-Learning*, 2017.
- Ricardo Baptista and Matthias Poloczek. Bayesian optimization of combinatorial structures. In *International Conference on Machine Learning*, pp. 462–471, 2018.
- J. Bergstra, R. Bardenet, Y. Bengio, and B. Kégl. Algorithms for hyper-parameter optimization. In J. Shawe-Taylor, R. Zemel, P. Bartlett, F. Pereira, and K. Weinberger (eds.), *Proceedings of the 25th International Conference on Advances in Neural Information Processing Systems (NIPS'11)*, pp. 2546–2554, 2011.
- Han Cai, Ligeng Zhu, and Song Han. Proxylessnas: Direct neural architecture search on target task and hardware. In *International Conference on Learning Representations*, 2019.
- Han Cai, Chuang Gan, Tianzhe Wang, Zhekai Zhang, and Song Han. Once-for-all: Train one network and specialize it for efficient deployment. In *International Conference on Learning Representations*, 2020. URL <https://openreview.net/forum?id=HylxE1HKwS>.
- Tianqi Chen and Carlos Guestrin. Xgboost: A scalable tree boosting system. In *Proceedings of the 22nd acm sigkdd international conference on knowledge discovery and data mining*, pp. 785–794, 2016.
- Liu Chenxi, Chen Liang Chieh, Schroff Florian, Adam Hartwig, Hua Wei, Yuille Alan L., and Fei Fei Li. Auto-deeplab: Hierarchical neural architecture search for semantic image segmentation. In *Conference on Computer Vision and Pattern Recognition*, 2019.
- Patryk Chrabaszcz, Ilya Loshchilov, and Frank Hutter. A downsampled variant of imagenet as an alternative to the cifar datasets. *arXiv preprint arXiv:1707.08819*, 2017.
- Boyang Deng, Junjie Yan, and Dahua Lin. Peephole: Predicting network performance before training. *arXiv preprint arXiv:1712.03351*, 2017.

-
- T. Dietterich. *Ensemble Methods in Machine Learning*, volume 1857 of *Lecture Notes in Computer Science*. Springer Berlin Heidelberg, 2000.
- T. Domhan, J. T. Springenberg, and F. Hutter. Speeding up automatic hyperparameter optimization of deep neural networks by extrapolation of learning curves. In Q. Yang and M. Wooldridge (eds.), *Proceedings of the 25th International Joint Conference on Artificial Intelligence (IJCAI’15)*, pp. 3460–3468, 2015.
- Xuanyi Dong and Yi Yang. Searching for a robust neural architecture in four gpu hours. In *Proceedings of the IEEE Conference on Computer Vision and Pattern Recognition (CVPR)*, pp. 1761–1770, 2019.
- Xuanyi Dong and Yi Yang. Nas-bench-102: Extending the scope of reproducible neural architecture search. In *International Conference on Learning Representations*, 2020. URL <https://openreview.net/forum?id=HJxyZkBKDr>.
- Vijay Prakash Dwivedi, Chaitanya K Joshi, Thomas Laurent, Yoshua Bengio, and Xavier Bresson. Benchmarking graph neural networks. *arXiv preprint arXiv:2003.00982*, 2020.
- K. Eggenberger, F. Hutter, H.H. Hoos, and K. Leyton-Brown. Efficient benchmarking of hyperparameter optimizers via surrogates. In B. Bonet and S. Koenig (eds.), *Proceedings of the Twenty-ninth National Conference on Artificial Intelligence (AAAI’15)*, pp. 1114–1120. AAAI Press, 2015.
- Thomas Elsken, Jan Hendrik Metzen, and Frank Hutter. Efficient multi-objective neural architecture search via lamarckian evolution. In *International Conference on Learning Representations*, 2019a.
- Thomas Elsken, Jan Hendrik Metzen, and Frank Hutter. Neural architecture search: A survey. *Journal of Machine Learning Research*, 20(55):1–21, 2019b.
- Federico Errica, Marco Podda, Davide Bacciu, and Alessio Micheli. A fair comparison of graph neural networks for graph classification. In *International Conference on Learning Representations*, 2020. URL <https://openreview.net/forum?id=HygDF6NFPB>.
- Stefan Falkner, Aaron Klein, and Frank Hutter. BOHB: Robust and efficient hyperparameter optimization at scale. In Jennifer Dy and Andreas Krause (eds.), *Proceedings of the 35th International Conference on Machine Learning*, volume 80 of *Proceedings of Machine Learning Research*, pp. 1437–1446, Stockholmsmässan, Stockholm Sweden, 10–15 Jul 2018. PMLR. URL <http://proceedings.mlr.press/v80/falkner18a.html>.
- Matthias Fey and Jan E. Lenssen. Fast graph representation learning with PyTorch Geometric. In *ICLR Workshop on Representation Learning on Graphs and Manifolds*, 2019.
- David Friede, Jovita Lukasik, Heiner Stuckenschmidt, and Margret Keuper. A variational-sequential graph autoencoder for neural architecture performance prediction. *ArXiv*, abs/1912.05317, 2019.
- Marco Gori, Gabriele Monfardini, and Franco Scarselli. A new model for learning in graph domains. In *Proceedings. 2005 IEEE International Joint Conference on Neural Networks, 2005.*, volume 2, pp. 729–734. IEEE, 2005.
- Kaiming He, Xiangyu Zhang, Shaoqing Ren, and Jian Sun. Deep Residual Learning for Image Recognition. In *CVPR*, 2016.
- Weihua Hu, Matthias Fey, Marinka Zitnik, Yuxiao Dong, Hongyu Ren, Bowen Liu, Michele Catasta, and Jure Leskovec. Open graph benchmark: Datasets for machine learning on graphs. *arXiv preprint arXiv:2005.00687*, 2020.
- Jenq-Neng Hwang, Shyh-Rong Lay, and Alan Lippman. Nonparametric multivariate density estimation: a comparative study. *IEEE Transactions on Signal Processing*, 42(10):2795–2810, 1994.
- Roxana Istrate, Florian Scheidegger, Giovanni Mariani, Dimitrios Nikolopoulos, Costas Bekas, and A Cristiano I Malossi. Tapas: Train-less accuracy predictor for architecture search. In *Proceedings of the AAAI Conference on Artificial Intelligence*, volume 33, pp. 3927–3934, 2019.

-
- Guolin Ke, Qi Meng, Thomas Finley, Taifeng Wang, Wei Chen, Weidong Ma, Qiwei Ye, and Tie-Yan Liu. Lightgbm: A highly efficient gradient boosting decision tree. In I. Guyon, U. V. Luxburg, S. Bengio, H. Wallach, R. Fergus, S. Vishwanathan, and R. Garnett (eds.), *Advances in Neural Information Processing Systems 30*, pp. 3146–3154. Curran Associates, Inc., 2017.
- Thomas N. Kipf and Max Welling. Semi-supervised classification with graph convolutional networks. In *International Conference on Learning Representations (ICLR)*, 2017.
- A. Klein, S. Falkner, J. T. Springenberg, and F. Hutter. Learning curve prediction with Bayesian neural networks. In *Proceedings of the International Conference on Learning Representations (ICLR’17)* icl (2017). Published online: iclr.cc.
- Nikita Klyuchnikov, Ilya Trofimov, Ekaterina Artemova, Mikhail Salnikov, Maxim Fedorov, and Evgeny Burnaev. Nas-bench-nlp: Neural architecture search benchmark for natural language processing. *arXiv preprint arXiv:2006.07116*, 2020.
- A. Krizhevsky. Learning multiple layers of features from tiny images. Technical report, University of Toronto, 2009.
- Balaji Lakshminarayanan, Alexander Pritzel, and Charles Blundell. Simple and scalable predictive uncertainty estimation using deep ensembles. In *Advances in neural information processing systems*, pp. 6402–6413, 2017.
- Gustav Larsson, Michael Maire, and Gregory Shakhnarovich. Fractalnet: Ultra-deep neural networks without residuals. In *ICLR*, 2017.
- Liam Li and Ameet Talwalkar. Random search and reproducibility for neural architecture search. In *Proceedings of the Thirty-Fifth Conference on Uncertainty in Artificial Intelligence, UAI 2019, Tel Aviv, Israel, July 22-25, 2019*, pp. 129, 2019. URL <http://auai.org/uai2019/proceedings/papers/129.pdf>.
- M. Lindauer, K. Eggenberger, M. Feurer, A. Biedenkapp, J. Marben, P. Müller, and F. Hutter. Boah: A tool suite for multi-fidelity bayesian optimization & analysis of hyperparameters. *arXiv:1908.06756 [cs.LG]*, 2019.
- Marius Lindauer and Frank Hutter. Best practices for scientific research on neural architecture search. *arXiv preprint arXiv:1909.02453*, 2019.
- Hanxiao Liu, Karen Simonyan, and Yiming Yang. DARTS: Differentiable architecture search. In *International Conference on Learning Representations*, 2019.
- I. Loshchilov and F. Hutter. Sgdr: Stochastic gradient descent with warm restarts. In *International Conference on Learning Representations (ICLR) 2017 Conference Track*, April 2017.
- Renqian Luo, Xu Tan, Rui Wang, Tao Qin, Enhong Chen, and Tie-Yan Liu. Neural architecture search with gbdt. *arXiv preprint arXiv:2007.04785*, 2020.
- Laurens van der Maaten and Geoffrey Hinton. Visualizing data using t-sne. *Journal of machine learning research*, 9(Nov):2579–2605, 2008.
- Niv Nayman, Asaf Noy, Tal Ridnik, Itamar Friedman, Rong Jin, and Lihi Zelnik. Xnas: Neural architecture search with expert advice. In H. Wallach, H. Larochelle, A. Beygelzimer, F. d Alché-Buc, E. Fox, and R. Garnett (eds.), *Advances in Neural Information Processing Systems 32*, pp. 1975–1985. Curran Associates, Inc., 2019.
- Xuefei Ning, Yin Zheng, Tianchen Zhao, Yu Wang, and Huazhong Yang. A generic graph-based neural architecture encoding scheme for predictor-based nas. *arXiv preprint arXiv:2004.01899*, 2020.
- Changyong Oh, Jakub Tomczak, Efstratios Gavves, and Max Welling. Combinatorial bayesian optimization using the graph cartesian product. In *Advances in Neural Information Processing Systems*, pp. 2910–2920, 2019.

-
- Fabian Pedregosa, Gaël Varoquaux, Alexandre Gramfort, Vincent Michel, Bertrand Thirion, Olivier Grisel, Mathieu Blondel, Peter Prettenhofer, Ron Weiss, Vincent Dubourg, et al. Scikit-learn: Machine learning in python. *Journal of machine learning research*, 12(Oct):2825–2830, 2011.
- Hieu Pham, Melody Y. Guan, Barret Zoph, Quoc V. Le, and Jeff Dean. Efficient neural architecture search via parameter sharing. *Arxiv*, 1802.03268, 2018.
- Kenneth Price, Rainer M Storn, and Jouni A Lampinen. *Differential evolution: a practical approach to global optimization*. Springer Science & Business Media, 2006.
- Esteban Real, Alok Aggarwal, Yanping Huang, and Quoc V Le. Regularized evolution for image classifier architecture search. In *Proceedings of the aaai conference on artificial intelligence*, volume 33, pp. 4780–4789, 2019.
- T. Saikia, Y. Marrakchi, A. Zela, F. Hutter, and T. Brox. Autodispnet: Improving disparity estimation with automl. In *IEEE International Conference on Computer Vision (ICCV)*, 2019. URL <http://lmb.informatik.uni-freiburg.de/Publications/2019/SMB19>.
- Han Shi, Renjie Pi, Hang Xu, Zhenguo Li, James T Kwok, and Tong Zhang. Multi-objective neural architecture search via predictive network performance optimization. *arXiv preprint arXiv:1911.09336*, 2019.
- Yao Shu, Wei Wang, and Shaofeng Cai. Understanding architectures learnt by cell-based neural architecture search. In *International Conference on Learning Representations*, 2020. URL <https://openreview.net/forum?id=BJxH22EKPS>.
- Christian Szegedy, Wei Liu, Yangqing Jia, Pierre Sermanet, Scott Reed, Dragomir Anguelov, Dumitru Erhan, Vincent Vanhoucke, and Andrew Rabinovich. Going deeper with convolutions. In *Computer Vision and Pattern Recognition (CVPR)*, 2015. URL <http://arxiv.org/abs/1409.4842>.
- Mingxing Tan, Bo Chen, Ruoming Pang, Vijay Vasudevan, and Quoc V. Le. Mnasnet: Platform-aware neural architecture search for mobile. *2019 IEEE/CVF Conference on Computer Vision and Pattern Recognition (CVPR)*, pp. 2815–2823, 2018.
- Yehui Tang, Yunhe Wang, Yixing Xu, Hanting Chen, Boxin Shi, Chao Xu, Chunjing Xu, Qi Tian, and Chang Xu. A semi-supervised assessor of neural architectures. In *Proceedings of the IEEE/CVF Conference on Computer Vision and Pattern Recognition (CVPR)*, June 2020.
- Wei Wen, Hanxiao Liu, Hai Li, Yiran Chen, Gabriel Bender, and Pieter-Jan Kindermans. Neural predictor for neural architecture search. *arXiv preprint arXiv:1912.00848*, 2019.
- Colin White, Willie Neiswanger, and Yash Savani. Bananas: Bayesian optimization with neural architectures for neural architecture search. *arXiv preprint arXiv:1910.11858*, 2019.
- Colin White, Willie Neiswanger, Sam Nolen, and Yash Savani. A study on encodings for neural architecture search. *arXiv preprint arXiv:2007.04965*, 2020a.
- Colin White, Sam Nolen, and Yash Savani. Local search is state of the art for nas benchmarks. *arXiv preprint arXiv:2005.02960*, 2020b.
- Zonghan Wu, Shirui Pan, Fengwen Chen, Guodong Long, Chengqi Zhang, and Philip S Yu. A comprehensive survey on graph neural networks. *arXiv preprint arXiv:1901.00596*, 2019.
- Keyulu Xu, Weihua Hu, Jure Leskovec, and Stefanie Jegelka. How powerful are graph neural networks? In *International Conference on Learning Representations*, 2019a. URL <https://openreview.net/forum?id=ryGs6iA5Km>.
- Yixing Xu, Yunhe Wang, Kai Han, Hanting Chen, Yehui Tang, Shangling Jui, Chunjing Xu, Qi Tian, and Chang Xu. Rnas: Architecture ranking for powerful networks. *ArXiv*, abs/1910.01523, 2019b.
- Yuhui Xu, Lingxi Xie, Xiaopeng Zhang, Xin Chen, Guo-Jun Qi, Qi Tian, and Hongkai Xiong. Pc-darts: Partial channel connections for memory-efficient architecture search. In *International Conference on Learning Representations*, 2020. URL <https://openreview.net/forum?id=BJ1S634tPr>.

-
- Antoine Yang, Pedro M Esperança, and Fabio M Carlucci. Nas evaluation is frustratingly hard. *arXiv preprint arXiv:1912.12522*, 2019.
- Chris Ying, Aaron Klein, Eric Christiansen, Esteban Real, Kevin Murphy, and Frank Hutter. NAS-bench-101: Towards reproducible neural architecture search. In Kamalika Chaudhuri and Ruslan Salakhutdinov (eds.), *Proceedings of the 36th International Conference on Machine Learning*, volume 97 of *Proceedings of Machine Learning Research*, pp. 7105–7114, Long Beach, California, USA, 09–15 Jun 2019. PMLR. URL <http://proceedings.mlr.press/v97/ying19a.html>.
- Kaicheng Yu, Rene Ranftl, and Mathieu Salzmann. How to train your super-net: An analysis of training heuristics in weight-sharing nas. *arXiv preprint arXiv:2003.04276*, 2020.
- Arber Zela, Thomas Elsken, Tonmoy Saikia, Yassine Marrakchi, Thomas Brox, and Frank Hutter. Understanding and robustifying differentiable architecture search. In *International Conference on Learning Representations*, 2020a. URL <https://openreview.net/forum?id=H1gDNyrKDS>.
- Arber Zela, Julien Siems, and Frank Hutter. Nas-bench-1shot1: Benchmarking and dissecting one-shot neural architecture search. In *International Conference on Learning Representations*, 2020b. URL <https://openreview.net/forum?id=SJx9ngStPH>.
- Hongyi Zhang, Moustapha Cisse, Yann N. Dauphin, and David Lopez-Paz. mixup: Beyond empirical risk minimization. *International Conference on Learning Representations*, 2018. URL <https://openreview.net/forum?id=r1Ddpl-Rb>.
- Jie Zhou, Ganqu Cui, Zhengyan Zhang, Cheng Yang, Zhiyuan Liu, Lifeng Wang, Changcheng Li, and Maosong Sun. Graph neural networks: A review of methods and applications. *arXiv preprint arXiv:1812.08434*, 2018.
- B. Zoph and Q. V. Le. Neural architecture search with reinforcement learning. In *Proceedings of the International Conference on Learning Representations (ICLR’17)* icl (2017). Published online: iclr.cc.

A APPENDIX

A.1 MOTIVATION - ALEATORIC UNCERTAINTY IN TABULAR BENCHMARKS

A.1.1 TRAINING DETAILS

We set the GIN to have a hidden dimension of 64 with 4 hidden layers which results in around $\sim 40k$ parameters. We trained for 30 epochs with a batch size of 128. We chose the MSE loss function and add a logarithmic transformation to emphasize the data fit on well performing architectures.

A.2 SURROGATE MODELS

A.2.1 PREPROCESSING OF THE GRAPH TOPOLOGY

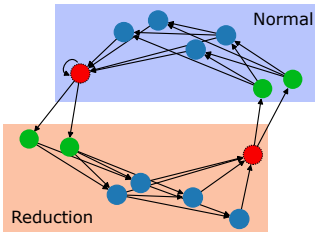


Figure 11: Architecture with inputs in green, intermediate nodes in blue and outputs in red.

DGN preprocessing All DGN were implemented using PyTorch Geometric (Fey & Lenssen, 2019) which supports the aggregation of edge attributes, hence we can naturally represent the DARTS architecture cells, by assigning the embedded operations to the edges. The nodes are labeled as input, intermediate and output nodes. We represent the DARTS graph as shown in Figure 11 in the appendix, by connecting the output node of each cell type with the inputs of the other cell, hence allowing information from both cells to be aggregated during message passing. Note the self-loop on the output node of the normal cell, which we found necessary to get the best performance.

Preprocessing for other surrogate models Since we make use of the framework implemented by BOHB (Falkner et al., 2018) to easily parallelize the architecture search algorithms across many compute nodes, we also represent our search space using ConfigSpace (Lindauer et al., 2019). For all non-DGN based surrogate models, we use the vector representation of a configuration given by ConfigSpace as input to the model.

A.3 DATA COLLECTION: NAS OPTIMIZER SETTINGS

In this section we provide the hyperparameters used for the evaluations of NAS optimizers for the collection of our dataset. Many of the optimizers require a specialized representation to work in the architecture space, because most of them are general HPO optimizers. As recently shown by White et al. (2020a), this representation can be critical for the performance of a NAS optimizer. Whenever the representation used by the Optimizer did not act directly on the graph representation, such as in RE, we detail how we represented it the architecture for the optimizer.

BANANAS We initialized BANANAS with 100 random architectures and modified the optimization of the surrogate model neural network, by adding early stopping based on a 90%/10% train/validation split and lowering the number of ensemble models to be trained from 5 to 3. These changes to bananas avoided a computational bottleneck in the training of the neural network.

COMBO COMBO only attempts to maximize the acquisition function when the entire initial design (100 architectures) has completed. For workers which are done before we sample a random architecture, hence increasing the initial design by the number of workers (30) we used for running the experiments. The search space regarded in our work is larger than all search spaces evaluated in COMBO (Oh et al., 2019) and we regard not simply binary architectural choices, as we have to make choices about pairs of edges. Hence, we increased the number of initial samples for ascent acquisition function optimization from 20 to 30. Unfortunately, the optimization of the GP already becomes the bottleneck of the BO after around 600 function evaluations, leading to many workers waiting for new jobs to be assigned.

Representation: In contrast to the NAS experiment in the COMBO paper, the DARTS search space has to make decisions based on pairs of parents of intermediate nodes where the number of choices

increase with the index of the intermediate nodes. The COMBO representation therefore consists of the graph cartesian product of the combinatorial choice graphs increasing in size with each intermediate node. In addition, there exists 8 choices over the number of parameters for the operation in a cell.

Differential Evolution DE was started with a generation size of 100. As the implementation was parallelized the workers would have to wait for a generation and its mutations to be completed for selection to start. We decided to keep the workers busy by training randomly sampled architectures in this case, as random architectures provide us good coverage of the space. But other methods using asynchronous DE selection would also be possible. Note, that the DE implementation by Awad et al. (2020), performs boundary checks and resamples components of an individual which exceed 1.0. We use the rand1 mutation operation which generally favors exploration over exploitation.

Representation: DE uses a vector representation for each individual in the population. Categorical choices are scaled to lie within the unit interval $[0, 1]$ and are rounded to the nearest category when converting back to the discrete representation in the implementation by Awad et al. (2020). Similarly to COMBO, we represent the increasing number of parent pair choices for the intermediate nodes by interpreting the respective entries to have an increasing number of sub-intervals in $[0, 1]$.

DARTS, GDAS, PC-DARTS and Random Search with Weight Sharing We collected the architectures found by all of the above one-shot optimizers with their default search hyperparameters. Several searches were performed for each one-shot optimizer.

RE To allow for a good initial coverage before mutations start, we decided to randomly sample 3000 architectures as initial population. RE then proceeds with a sample size of 100 to extract well performing architectures from the population and mutates them. During mutations RE first decides whether to mutate the normal or reduction cell and then proceeds to perform either a parent change, an operation change or no mutation.

TPE For TPE we use the default settings as also used by BOHB. We use the Kernel-Density-Estimator surrogate model and build two models where the good configs are chosen as the top 15%. The acquisition function expected improvement is optimized by sampling 64 points.

A.4 TRAINING DETAILS

Each architecture was evaluated on CIFAR-10 (Krizhevsky, 2009) using the standard 40k, 10k, 10k split for train, validation and test set. The networks were trained using SGD with momentum 0.9, initial learning rate of 0.025 and a cosine annealing schedule (Loshchilov & Hutter, 2017) annealing towards 10^{-8} . For data augmentation, we used CutOut (Loshchilov & Hutter, 2017) with cutout length 16 and MixUp (Zhang et al., 2018). For regularization, we used an auxiliary tower (Szegedy et al., 2015) with a weight of 0.4 and DropPath (Larsson et al., 2017) with drop probability of 0.2. We trained each architecture for 100 epochs with a batch size of 96, using 32 initial channels and 8 cell layers. We chose these values to be close to the proxy model used by DARTS while achieving good performance.

A.5 DATA STATISTICS

A.5.1 T-SNE ANALYSIS FOR DIFFERENT OPTIMIZERS

We find that RE discovers well-performing architectures which form clusters distinct from the architectures found via RS. We observe that COMBO searched previously unexplored areas of the search space. BANANAS, which found some of the best architectures, explores clusters outside the main embedding space. However, it heavily exploits regions, instead of exploring. We argue that this is a result of the optimization of the acquisition function via random mutations based on the previously found iterates, rather than new random architectures. DE is the only optimizer which finds well performing architectures in the center of the embedding space.

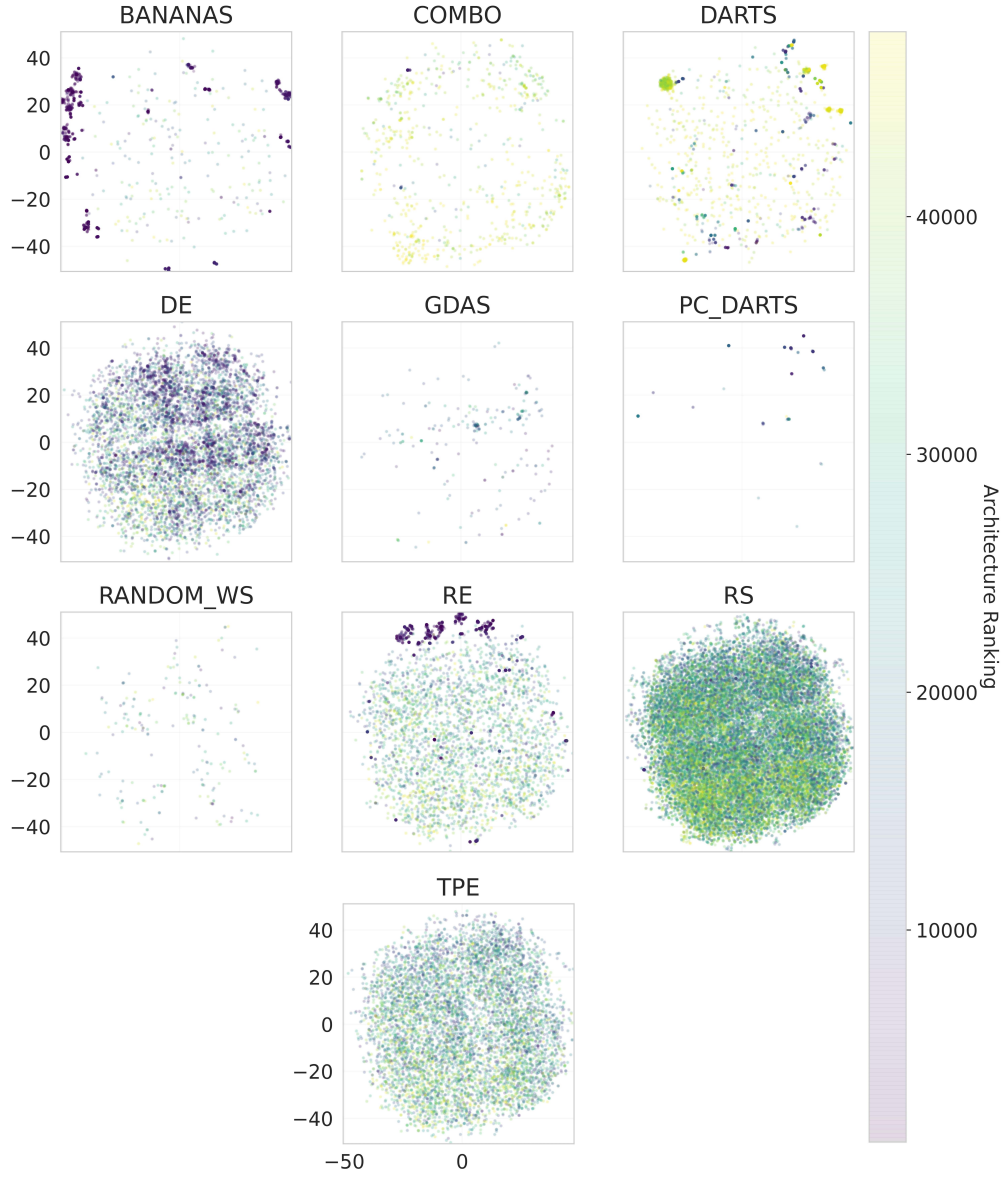


Figure 12: Visualization of the exploration of different parts of the architectural t-SNE embedding space for all optimizers used for data collection. The architecture ranking is global over the entire data collection of all optimizers.

A.5.2 CELL TOPOLOGY AND OPERATIONS

In Figure 13 we show how the t-SNE projection captured the cell depth as the structural property well, further validating that we covered the search space well.

We also show the distribution of normal and reduction cell depths of each optimizer in Figure 14 to get a sense of the differences between the discovered architectures. We observe that DARTS and BANANAS generally find architectures with shallow reduction cell and deeper normal cell, while the reverse is true for RE. DE, TPE, COMBO and RS appear to find normal and reduction cell with similar cell depth.

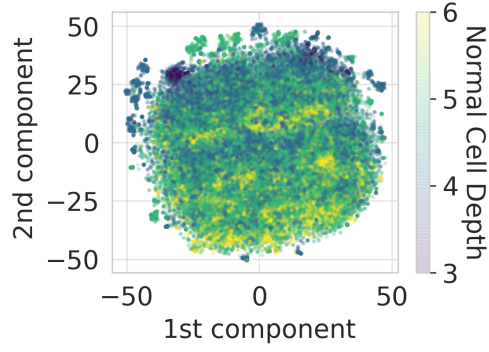


Figure 13: Normal Cell Depth

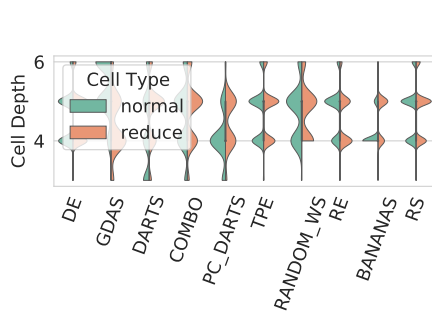


Figure 14: Comparison between the normal and reduction cell depth for the architectures found by each optimizer.

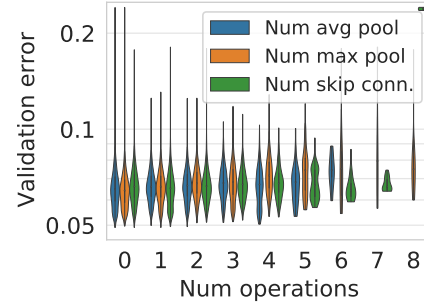


Figure 15: Distribution of validation error in dependence of the number of parameter-free operations in the reduction cell. Violin plots are cut off at the respective observed minimum and maximum value.

In the reduction cell, the number of parameter-free operations has less effect as shown in Figure 15. In contrast to the normal cell where 2-3 skip-connections in a normal cell lead to generally better performance the reduction cell shows no similar trend.

A.6 DETAILS ON HPO

Model	Hyperparameter	Range	Log-transform	Default Value
GIN	Hidden dim.	[16, 256]	true	24
	Num. Layers	[2, 10]	false	8
	Dropout Prob.	[0, 1]	false	0.035
	Learning rate	[1e-3, 1e-2]	true	0.0777
	Learning rate min.	Const.	-	0.0
	Batch size	Const.	-	51
	Undirected graph	[true, false]	-	false
	Pairwise ranking loss	[true, false]	-	true
	Self-Loops	[true, false]	-	false
	Loss log transform	[true, false]	-	true
	Node degree one-hot	Const.	-	true
BANANAS	Num. Layers	[1, 10]	true	17
	Layer width	[16, 256]	true	31
	Dropout Prob.	Const.	-	0.0
	Learning rate	[1e-3, 1e-1]	true	0.0021
	Learning rate min.	Const.	-	0.0
	Batch size	[16, 128]	-	122
	Loss log transform	[true, false]	-	true
XGBoost	Pairwise ranking loss	[true, false]	-	false
	Early Stopping Rounds	Const.	-	100
	Booster	Const.	-	gbtree
	Max. depth	[1, 15]	false	13
	Min. child weight	[1, 100]	true	39
	Col. sample bylevel	[0.0, 1.0]	false	0.6909
	Col. sample bytree	[0.0, 1.0]	false	0.2545
	lambda	[0.001, 1000]	true	31.3933
	alpha	[0.001, 1000]	true	0.2417
	Learning rate	[0.001, 0.1]	true	0.00824
LGBBoost	Early stop. rounds	Const.	-	100
	Max. depth	[1, 25]	false	18
	Num. leaves	[10, 100]	false	40
	Max. bin	[100, 400]	false	336
	Feature Fraction	[0.1, 1.0]	false	0.1532
	Min. child weight	[0.001, 10]	true	0.5822
	Lambda L1	[0.001, 1000]	true	0.0115
	Lambda L2	[0.001, 1000]	true	134.5075
	Boosting type	Const.	-	gbdt
Random Forest	Learning rate	[0.001, 0.1]	true	0.0218
	Num. estimators	[16, 128]	true	116
	Min. samples split.	[2, 20]	false	2
	Min. samples leaf	[1, 20]	false	2
	Max. features	[0.1, 1.0]	false	0.1706
ϵ -SVR	Bootstrap	[true, false]	-	false
	C	[1.0, 20.0]	true	3.066
	coef. 0	[-0.5, 0.5]	false	0.1627
	degree	[1, 128]	true	1
	epsilon	[0.01, 0.99]	true	0.0251
	gamma	[scale, auto]	-	auto
	kernel	[linear, rbf, poly, sigmoid]	-	sigmoid
	shrinking	[true, false]	-	false
μ -SVR	tol	[0.0001, 0.01]	-	0.0021
	C	[1.0, 20.0]	true	5.3131
	coef. 0	[-0.5, 0.5]	false	-0.3316
	degree	[1, 128]	true	128
	gamma	[scale, auto]	-	scale
	kernel	[linear, rbf, poly, sigmoid]	-	rbf
	nu	[0.01, 1.0]	false	0.1839
	shrinking	[true, false]	-	true
	tol	[0.0001, 0.01]	-	0.003

Table 6: Hyperparameters of the surrogate models and the default values found via HPO.

A.6.1 HPO FOR RUNTIME PREDICTION MODEL

Our runtime prediction model is an LGB model trained on the runtimes of architecture evaluations of DE. This is because we partially evaluated the architectures utilizing different CPUs. Hence, we only choose to train on the evaluations carried out by the same optimizer on the same hardware to

keep a consistent estimate of the runtime. DE is a good choice in this case, because it both explored and exploited the architecture space well. The HPO space used for the LGB runtime model are the same as used for the LGB surrogate model.